Applied Energy 184 (2016) 605–618

Contents lists available at ScienceDirect

Applied Energy

journal homepage: www.elsevier.com/locate/apenergy

Optimal energy-efficient predictive controllers in automotive air-conditioning/refrigeration systems

Yanjun Huang [a,*], Amir Khajepour [a], Farshid Bagheri [b], Majid Bahrami [b]

[a] Department of Mechanical and Mechatronics Engineering, University of Waterloo, Ontario N2L3G1, Canada
[b] School of Mechatronic System Engineering, Simon Fraser University, Surry, BC V3T 0A3, Canada

HIGHLIGHTS

- A discrete MPC is designed for the A/C-R system with a three-speed compressor.
- The control performance is studied under both normal and frosting conditions.
- Two designed hybrid controllers are more efficient under any heating load condition.
- A continuous MPC is made for the A/C-R system with continuously varying components.
- The controllers bring better performance and save up to 23% energy for A/C-R systems.

ARTICLE INFO

Article history:
Received 10 August 2016
Received in revised form 14 September 2016
Accepted 26 September 2016
Available online 10 November 2016

Keywords:
Air-conditioning/refrigeration systems
Frosting
Discrete MPC
Robust MPC
Hybrid controller

ABSTRACT

This paper presents several robust model predictive controllers that improve the temperature performance and minimize energy consumption in an automotive air-conditioning/refrigeration (A/C-R) system with a three-speed and continuously-varying compressor. First, a simplified control-oriented model of the A/C-R system is briefly introduced. Accordingly, a discrete Model Predictive Controller (MPC) is designed based on the proposed model for an A/C-R system with a three-speed compressor. A proper terminal weight is chosen to guarantee its robustness under both regular and frost conditions. A case study is conducted under various heating load conditions. Two hybrid controllers are made, which combine the advantages of both the on/off controller and discrete MPC such that they will be more efficient under any ambient heating condition. In addition, a continuous MPC is developed for systems with continuous variable components. Finally, the experimental and simulation results of the new controllers and the conventional on/off controller are provided and compared to show that the proposed controllers can save up to 23% more energy.

1. Introduction

The continuously increasing demands on energy conservation and environmental protection have driven researchers to develop more efficient and "green" vehicles [1,2]. Recently, A/C-R systems have been widely used as the main auxiliary devices in vehicles. For example, A/C-R systems in food delivery trucks consume up to 25% of the vehicle's total fuel consumption. Efficiently operating A/C-R systems can significantly improve operating costs and the vehicle's effects on the environment [3,4]. Thus, making more efficient auxiliary devices such as A/C-R systems can bring many benefits to vehicle owners as well as the environment [5]. For any A/C-R system, a foremost step in achieving better performance and higher energy efficiency is a proper control strategy. However, in most conventional vehicles, the compressor speed is proportional to the engine speed instead of actively varying with the requirements of passengers or working conditions. This impedes the development of advanced controllers for A/C-R systems given that the controllers are usually applied to manipulate the speeds of the compressor and fans of heat exchangers. Recently, the onboard energy storage system (ESS) of anti-idling systems [6], hybrid electric vehicles (HEVs) [7] and electric vehicles (EV) [8,9] is capable of powering the A/C-R system independently such that the A/C-R system can be disconnected from the engines [10]. This indicates the feasibility of the electrification of the A/C-R system and the subsequent application of advanced controllers in vehicles. For the sake of accurate prediction, an accurate yet simple dynamic model of the whole A/C-R system is a prerequisite for the design of

* Corresponding author.
E-mail addresses: y269huan@uwaterloo.ca (Y. Huang), a.khajepour@uwaterloo.ca (A. Khajepour), fbagheri@sfu.ca (F. Bagheri), mbahrami@sfu.ca (M. Bahrami).

http://dx.doi.org/10.1016/j.apenergy.2016.09.086
0306-2619/

Nomenclature

A_v	opening area of expansion valve
$A_c(A_e)$	cross-sectional area of condenser (evaporator) tube
$A_{oc}(A_{oe})$	exterior area of the condenser (evaporator)
$\alpha_{ic}(\alpha_{ie})$	equivalent refrigerant-side heat transfer coefficient in two-phase region
$\alpha_{oc}(\alpha_{oe})$	air-side heat transfer coefficient
$\alpha_{icsh}(\alpha_{iesh})$	refrigerant-side heat transfer coefficient in superheat region
C_p	specific heat of the heat exchangers
C_v	discharge coefficient of expansion valve
C_{air}	specific heat of the ambient air
$D_{ic}(D_{ie})$	heat exchanger tube internal diameter
$h_{ge}(h_{gc})$	enthalpy of vapor refrigerant
$h_{ic}(h_{ie})$	enthalpy of refrigerant at the inlet of heat exchanger
h_{is}	isentropic of refrigerant in compressor
$h_{lc}(h_{le})$	enthalpy of liquid refrigerant
$h_{lgc}(h_{lge})$	latent enthalpy of refrigerant
h_{oc}	enthalpy at the outlet of condenser
$l_c(l_e)$	length of two-phase section in two heat exchangers
$\dot{m}_v$	refrigerant mass flow rate through the expansion valve
$\dot{m}_{comp}$	refrigerant mass flow rate through the compressor
m_{pipe}	total refrigerant mass in the pipes
m	heat exchanger total mass
N_{comp}	compressor speed
N_{cond}	condenser fan control input
N_{evap}	evaporator fan control input
$P_c(P_e)$	pressure of two heat exchangers
ρ_v	density of refrigerant through the valve
ρ_{ref}	density of refrigerant
$\rho_{lc}(\rho_{le})$	density of liquid refrigerant
$\rho_{gc}(\rho_{ge})$	density of vapor refrigerant
$\rho_{shc}(\rho_{she})$	density of refrigerant in superheat section
T_{amb}	ambient temperature
$T_{wfc}(T_{wfe})$	equivalent temperature of tube wall & fin
$T_{rc}(T_{re})$	saturation temperature of refrigerant
$T_{ac}(T_{ae})$	air temperature around the heat exchanger
T_{sh}	superheat
T_{ic}	refrigerant temperature at the inlet of condenser
T_{cargo}	temperature of cargo
T_{cargo_init}	initial temperature of cargo
V_d	volumetric displacement of compressor
η_{vol}	volumetric efficiency of compressor
η_a	adiabatic efficiency of compressor
$\bar{\gamma}_c(\bar{\gamma}_e)$	mean void fraction of two-phase section
N	prediction and control horizontal length
P, Q, S	weight factor

any advanced controller. A simplified control-based model for all-purpose A/C-R systems that is validated by experimental data is provided [11]. Further based on the model, the controllers' development process is presented and followed by experimental validation and comparison work.

A literature review on the existing controllers including the MPC of A/C-R systems and the novelties of this paper is presented in the second section; next, the simplified model is briefly introduced. A brief introduction of the experimental system is provided in the following section. In addition, the development and implementation process of controllers are elaborated upon. Furthermore, the experimental results of both the discrete MPC and the conventional on/off controller are provided to demonstrate the energy-saving ability and the robustness of the proposed MPC. Moreover, a case study under varying heating load conditions is conducted by proposing the hybrid MPCs and the continuous MPC. In the last section, comments and future work are discussed.

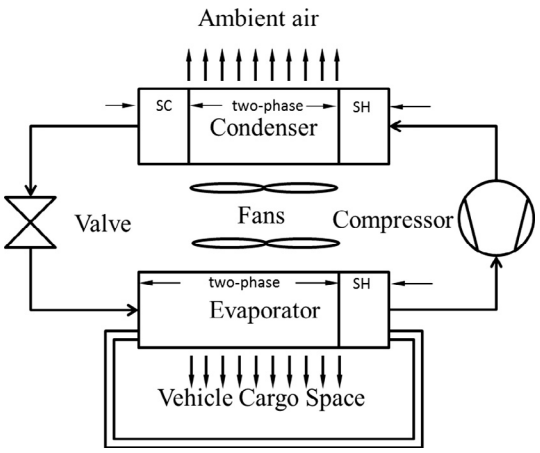

Fig. 1. Schematic diagram of an automotive A/C-R system with cargo.

2. Literature review

The A/C-R system generally consists of four main components: the compressor, evaporator, expansion valve, and the condenser, as shown in Fig. 1. One cycle is taken as an example for the demonstration of the whole working process of the A/C-R system. Let us begin with the high-pressure and low-temperature liquid refrigerant after it exits the condenser. It stays in the liquid phase before entering the expansion valve. Since the valve is usually assumed to be adiabatic, the enthalpy of the refrigerant at the inlet and outlet of the valve should be equal. In the evaporator, the low temperature and low-pressure two-phase refrigerant absorbs heat from the cargo space and exits from the superheat (SH) section in gas form to avoid damaging the compressor. The gas refrigerant is pressed when going through the compressor and exits the compressor with high temperature and high pressure. Finally, when it reaches the condenser, the superheated and over pressured gas refrigerant will go through the SH, two-phase and subcooling (SC) section when flowing through the condenser. Due to the extensive applications of A/C-R systems in different areas, many controllers have been developed in the literature.

Thanks to its simplicity, the on/off controller was initially applied. It could maintain the required temperature in a certain range by turning the whole system on or off. Instead, the on/off controller has many limitations. First, it is unable to regulate the temperature oscillation amplitudes in changing conditions including changing ambient temperatures or varying food temperatures. Secondly, frequent compressor activations (turning it on/off) can lead to excessive power consumption and cause the mechanical components to wear down over time. Above all, energy efficiency is not considered at all, and that is why [12,13] improved the original on/off controller's efficiency by introducing adaptive or optimization algorithms. However, due to the nature of the on/off controller, it is impossible to greatly enhance its performance. Recently, the application of variable-speed components into the

A/C-R system makes the development of more efficient controllers possible. Particularly, as anti-idling technologies and electric vehicles become more popular, the electrification technology of the A/C-R system in the vehicle will separate the compressor from the engine, which could make compressor actively change its speed instead of passively following the engine's speed. The current controllers (other than the on/off one of the A/C-R system) can be classified into three types [14]: classic feedback controller, intelligent controller, and advanced controller. As the most popular type of conventional feedback controllers, the PID controller has been used for a long time. A relevant example is the superheat-expansion valve and temperature-compressor control [15]. That means the superheat will be controlled by the expansion valve, and the temperature will be controlled by the compressor via two separate PID controllers. Nevertheless, due to the nonlinear and MIMO nature of an A/C-R system, it is difficult to find and tune the controller parameters [16]. A strategy used to decouple the controllers was developed in [17]. Still, this conventional PID controller does not directly consider saving energy.

Artificial intelligent control approaches, such as artificial neural network (ANN) control, fuzzy logic control, and the expert system, are utilized to deal with nonlinearities or uncertainties in A/C-R processes. ANN has a strong modeling capability for nonlinearities; whereas, fuzzy logic can deal with uncertainties in a straightforward manner. Besides being used directly as controllers based on their own formulation characteristics, ANN, fuzzy logic, etc., also perform the roles of A/C-R models [18], computing methods, and approximations of other control algorithms. In some cases, these artificial intelligent control approaches are combined with the A/C-R system control [14]. However, their limitations were discussed in [19], which comprise over training, extrapolation, network optimization, and the lack of optimal controls. These drawbacks impede its development and application.

Advanced control generally includes robust control (e.g. Sliding Model Control), adaptive control, optimal control (such as the MPC), and so on. A second-order Sliding Mode Controller (SMC) for the SISO refrigeration system was presented in [20], which regulates the refrigerant's relative length in the evaporator by manipulating the compressor speed. This controller can also effectively alleviate chattering phenomenon, but it does not deal with power consumption directly. A multivariable adaptive controller was proposed in [21], which is able to identify different linear models for a nonlinear system over the domain of operating conditions. There are also other classes of nonlinearity compensation controls like robust control [22], gain scheduling LQR [23,24] and optimizing control [25].

In all of these advanced control methods, the MPC is a more successful and promising control algorithm based on studies of model identification, optimized algorithm, control structure analysis, parameter tuning, and relevant stability and robustness. In A/C-R system control, the MPC is gradually becoming a major control method. The main value of the MPC is its ability to control multivariable systems under various constraints, especially slow dynamic plants, in an optimal way. It can simultaneously control more than one objective to achieve multi-objective and multivariable control; these variables include air temperature, relative humidity, the decrease of operation cost (e.g. energy saving), the improvement of air quality, and enhancement of steady-state performance and robustness. A comprehensive literature review was conducted in [16] on the theory and applications of controllers. In particular, they focused on the MPC in the HVAC systems of buildings, and they elaborated upon the factors that influence the performance of the MPC such as controller structure, process type, optimization algorithms, plant model, prediction horizon, control horizon, constraints, and an objective function. A Takagi-Sugeno fuzzy model was used to represent the highly nonlinear HVAC system in temperature predictive control. In order to reduce the computational effort of the non-convex optimization problem, a combination of a branch-and-bound search technique was used [26]. A hierarchical multiple MPC was proposed for the temperature control of the HVAC system based on a Takagi–Sugeno fuzzy model [27]. Authors in [28] have applied a neuro-predictive controller for the temperature control of automotive air conditioning systems. However, the conclusions are tenuous without any supporting experimental work. Literature [29] designed a MPC for a multi-evaporator vapor compression cooling cycle. A decentralized control structure was employed where the global MPC was to find the set points of the required cooling as well as evaporator pressures and local PI controllers were used for set-point tracking. By properly controlling evaporator pressures and superheat, energy efficiency can be improved. Authors in [30] used a neuro-fuzzy network based offline optimization to approximate the input-output relationship of a robust MPC, and validated it on an air-handling unit for the temperature control to increase the computational efficiency of a nonlinear robust MPC. An exergy-based objective function was incorporated into a nonlinear MPC to improve the coefficient of performance (COP) of a vapor-compressor cycle operation [31]. Due to the nonlinear objective function, the "*fmincon*" command in MATLAB that was used for the simulation and real-time implementation is not feasible in practice due to its high computational time. J. Ma et al. proposed an economic MPC to reduce costs for building HVAC systems. In each time interval, a min-max optimization technique is used and transferred to a linear programming problem instead of solving the optimization problem directly; this technique minimizes electricity costs and finds the optimal input for the next step [32]. In [33], the author adopted a complex nonlinear model of a vapor compressor system derived by [23], linearized it and subsequently designed a MPC to control the evaporator pressure and superheat by manipulating the compressor speed and electronic expansion valve. The purpose of this MPC was to improve the energy efficiency of the overall plant. In order to show its performance in real situations, several scenarios were simulated by using the linearized mode, but this was done without any experimental validation. In addition, the effects of model inaccuracy on the controller were not studied. An MPC was designed for a commercial multi-zone refrigeration system to minimize the total energy consumption, which employed a fast convex quadratic programming solver to solve a sequential convex optimization problem so as to handle the non-convexity of the objective function. In order to limit the size of the optimization problem in each step, a sample time of 15 min was chosen for predictions of the next 24 h [34]. A low-complexity MPC was developed for building cooling systems with thermal energy storage. In order to improve the computational efficiency, a periodic moving window blocking strategy is utilized [35]. A time-varying periodic robust invariant set discussed in [36] was used as the terminal constraint to guarantee the robustness under the time-varying uncertain cooling demand. The running time for each step was about 20mins, which satisfies the sample time of 1 h chosen for the MPC for prediction of the next 24 h. A learning-based MPC was proposed in [37] to minimize the energy consumption of an air conditioner while it maintains a comfortable temperature at the same time. A statistical method and a mathematical model for the temperature dynamics of a room were used to learn about the time-varying heating load caused by occupants and equipment. Based on the information learned from the heating load, this MPC will determine the state (on/off) of the air conditioner. Ultimately, it is still a two position controller for the air conditioner, but it is more intelligent. The authors improved their study discussed in [29]. A multi-evaporator vapor compression system was still the research target and the global MPC was used to find the required cooling and pressure set points for each zone. The local MPCs

and PIDs for each evaporator were used to track these set points by manipulating the valve position and evaporator fan speed. Energy efficiency was guaranteed by choosing the proper pressures and superheats instead of directly integrating the system's inputs into the objective functions of the MPC [38]. An adaptive MPC for a reefer container was proposed in [39]. Model parameters, states as well as the ambient temperature information for the next 24 h were identified online. This long prediction period required a relatively long time interval of 1 h to reduce the optimization problem size at each time step so as to guarantee the real-time application. Since the MPC is recalculated once every hour, the cooling provided by the refrigeration system could be incorrect for up to one hour. This MPC is not suitable for reefer containers in delivery trucks with small thermal inertia since such trucks unload their goods regularly resulting in some extra heating load in the container, which can ruin the quality of the goods. Due to the small thermal inertia and subsequent fast thermal dynamics, the 1 h time interval is too large to be used.

Compared to the aforementioned literature, the differences of this paper are as follows: (1) from the application point of view, this paper proposes a robust real-time MPC controller for automotive A/C-R systems. Most of the MPC applications of A/C-R systems in the existing literature are designed for buildings rather than for vehicles because the compressor, the most energy-consuming component in the A/C-R system, is directly connected to engine in conventional vehicles. The fact that its speed cannot be freely changed impedes the applications of advanced controllers. As HEVs, EVs, and anti-idling techniques become more popular, the electrification of the A/C-R systems and application of the MPC is possible. In addition, buildings with large thermal inertia present extremely slow temperature dynamics in which time intervals in minutes or even hours [16,35,37–39] are used in the controller loops. Vehicles with small passenger compartment, relatively poor insulation conditions reflect a relatively fast thermal dynamics, which calls for a smaller time interval, so controllers with real-time implementation potential are required. Our work in this paper introduces an MPC for A/C-R systems that satisfies the requirements for vehicle applications. (2) Regarding the model used for MPC development, neither the intelligent artificial [26–28,30] nor the data-driven modeling method is utilized. In this paper, the boundary-moving and lumped parameter method [22,23] is adopted according to the physical structure and characteristics of the plant. This method does not need any training work. Using an online parameter identification algorithm, the proposed model is sufficient to guarantee a better prediction accuracy required by the MPC over the models used in the literature. In addition, as opposed to complex models with more than fifteen states developed in the literature [13,22,23], this paper uses a simplified six-state control-oriented model with comparable accuracy. This has been done by introducing the effects of fins and superheat sections in the model [11]. (3) In terms of the controller itself, due to the discrete nature of the constraints in many A/C-R systems [25,40–42] a discrete MPC is proposed, which is rarely mentioned in the current literature about A/C-R systems. Thanks to the simple model, this controller is fast enough to be applied in real time. The design process of this discrete MPC can serve as a framework for other similar applications with several discrete points. Furthermore, the hybrid controllers combine the advantages of both the MPC and the on/off controller to make more efficient controllers under any heating load condition. Above all, concerning the robustness of the proposed MPC, as is suggested by [43,44] a relatively large terminal weight is experimentally tested and chosen for the sake of robustness. The control performance is studied under both large external disturbances and situations of model parameter uncertainties. A 200-s heating load—up to 23% of the original heating load as the external disturbance is applied to the system to evaluate the robustness of the controller. Frosting, a common phenomenon in A/C-R systems, can lead to model inaccuracy, or even violate the assumptions of the modeling. However, even under such harsh situations, the control system shows an excellent performance because of the robustness of the proposed controller; whereas, the existing literature seldom shows the performance of controllers during the frosting period of the A/C-R system.

3. Modeling of A/C-R systems

The development of advanced controllers is usually based on a dynamic model, which should be simple enough for real-time applications and reflect the main dynamics of the plant. In this section, the dominant equations of the four main components of the A/C-R system are provided and explained, for more detailed information please the previous work [11].

3.1. Expansion valve

The expansion valve is assumed to be isenthalpic i.e. the enthalpy at the inlet of the valve is identical to that at the outlet. No matter which kind of expansion valve, the refrigerant mass flow rate $\dot{m}_v$ through the expansion valve is modeled by:

$$\dot{m}_v = C_v A_v \sqrt{\rho_v (P_c - P_e)} \tag{1}$$

For different types of expansion valves, the discharge coefficient C_v and valve opening area A_v have different correlations obtained by experimental data [45,46] P_c and P_e are the pressure of condenser and evaporator, respectively.

3.2. Compressor model

The dynamics of the compressor can be demonstrated by:

$$\dot{m}_{comp} = N_{comp} V_d \eta_{vol} \rho_{ref}(P_e) \tag{2}$$

$$h_{oc} = \eta_a (h_{is}(P_e, P_c) - h_{ic}(P_e)) + h_{ic}(P_e) \tag{3}$$

Eq. (2) depicts the refrigerant mass flow rate throughout the compressor with respect to the compressor speed, and Eq. (3) shows the enthalpy change of the refrigerant after going through the compressor.

3.3. Evaporator

Two common types of heat exchangers are used in the A/C-R system: the microchannel type and the fin-tube type [47]. The modeling method proposed is suitable for any type. More importantly, the modeling method takes the fins' effect into consideration and lumps it into two equivalent parameters so that the model is simple but accurate. The simplified nonlinear dynamic model of the evaporator can be written as:

$$h_{lge}\rho_{le}(1-\bar{\gamma}_e)A_e \frac{dl_e}{dt} = \dot{m}_v(h_{ge} - h_{ie}) - \alpha_{ie}\pi D_{ie} l_e (T_{wfe} - T_{re}) \tag{4}$$

$$A_e L_e \frac{d\rho_{ge}}{dP_e}\frac{dP_e}{dt} = \dot{m}_v \frac{h_{ie} - h_{le}}{h_{lge}} - \dot{m}_{comp} + \frac{\alpha_{ie}\pi D_{ie} l_e (T_{wfe} - T_{re})}{h_{lge}} \tag{5}$$

$$(C_p m)_{wfe}\frac{dT_{wfe}}{dt} = \alpha_{oe}A_{oe}(T_{ae} - T_{wfe}) - \alpha_{ie}\pi D_{ie} l_e (T_{wfe} - T_{re}) - \alpha_{iesh}\pi D_{ie}(L_e - l_e)(T_{wfe} - T_{re}) \tag{6}$$

where the three states are the length l_e of the two-phase section, the pressure P_e of the evaporator, and equivalent temperature T_{wfe} of tube wall & fins. Eq. (4) simulates the energy transfer from the refrigerant to the heat exchanger tube wall & fins of the

two-phase section [24]. Eq. (5) denotes the vapor refrigerant change rate throughout the evaporator tube. Eq. (6) reflects the heat conduction of the entire heat transfer process. The last term on the right-hand side represents the heat conduction throughout the superheat section, which is added to improve model accuracy and distinguish it from the model proposed in [23,24]. α_{oe} is regulated by the evaporator fan speed N_{evap} [22].

3.4. Condenser

As is known, the total mass m_{total} of the refrigerant inside the cycle is constant without considering any leakage. The mass of the refrigerant outside of the two heat exchangers is defined as m_{pipe}. Thus, the difference between these two masses is the mass inside evaporator and condenser, which can be shown by:

$$m_{total} - m_{pipe} = A_e\left[\rho_{le} l_e(1-\bar{\gamma}_e) + \rho_{ge} l_e \bar{\gamma}_e + \rho_{she}(L_e - l_e)\right] + A_c\left[\rho_{lc} l_c(1-\bar{\gamma}_c) + \rho_{gc} l_c \bar{\gamma}_c + \rho_{shc}(L_c - l_c)\right] \quad (7)$$

With the same modeling method, the condenser dynamics can be represented by the following two-state model by considering Eq. (7),

$$A_c L_c \frac{d\rho_{gc}}{dP_c}\frac{dP_c}{dt} = \dot{m}_{comp} - \frac{\alpha_{ic}\pi D_{ic} l_c (T_{rc} - T_{wfc})}{h_{lgc}} \quad (8)$$

$$(C_p m)_{wfc}\frac{dT_{wfc}}{dt} = \alpha_{oc}(N_{cond})A_{oc}(T_{ac} - T_{wfc}) - \alpha_{ic}\pi D_{ic} l_c (T_{wfc} - T_{rc}) - \alpha_{icsh}\pi D_{ic}(L_c - l_c)\left(T_{wfc} - (T_{rc} + T_{ic})/2\right) \quad (9)$$

3.5. Cargo

The inside temperature of the cargo is one of the control objectives, whose dynamics can be shown by the following equation:

$$\frac{dT_{cargo}}{dt} = \frac{\dot{Q}_{inconv} + \dot{Q}_{inf} + \dot{Q}_{door} - \dot{Q}_{vcc}}{(MC)_{air}} \quad (10)$$

where $\dot{Q}_{inconv}$ represents the convective heat transfer from the interior surface; $\dot{Q}_{inf}$ and $\dot{Q}_{door}$ are the load due to infiltration and opening the door respectively, and $\dot{Q}_{vcc}$ is the cooling capacity produced by the A/C-R system to balance the heating load from outside [48,49]. The first two loads will be treated together ($\dot{Q}_{out}$), and they can be identified by test data obtained from the previous step. $\dot{Q}_{door}$ is used as an external disturbance and added to the chamber.

By considering the boundary conditions of each component and integrating the cargo into the whole cycle, the entire model will become a six-state dynamic model. In this model, the air temperature T_{amb} at the inlet of the condenser is considered to be the ambient air temperature, and it is a measured value. The system inputs are compressor speed N_{comp} as well as the frequencies (N_{evap} and N_{cond}) of two variable frequency drives (VFDs) used to manipulate the speed of the evaporator and condenser fans. The frequencies are proportional to the two fan speeds. The six states $[P_e, P_c, l_e, T_{wfe}, T_{wfc}, T_{cargo}]$ are: pressures of the evaporator and the condenser, the two-phase section lengths, equivalent tube wall & fins temperatures of two heat exchangers, and the temperature of the evaporator-side temperature, respectively. The output is the air temperature T_{cargo} of the cargo.

4. Experimental system

In order to validate the model and verify the performance of these new controllers, an automotive A/C-R system is built. From the schematic of the experimental system in Fig. 2, it can be seen that two independent environmental chambers are connected to the evaporator and condenser units by pipes. The evaporator-side chamber acts as the cargo and its temperature will be a controlled parameter while the temperature at the inlet of the condenser can be controlled and used as operating conditions when the experiments are conducted.

The experimental setup is shown in Fig. 3, where the four main components of the whole system and the two chambers are labeled. Fig. 4 shows one of the environmental chambers. The Micro Motion 2400S transmitter with 0.5% accuracy from Emerson Electric Co. is utilized to log the refrigerant mass flow rate, and it is located between the condenser and the thermostatic expansion valve given in Fig. 5. The T-type thermocouples and pressure transducers model PX309 manufactured by OMEGA with 0.25% accuracy shown in Fig. 6 are installed at four locations of the whole system to measure both the high and low temperatures/pressures of the refrigerant. Fig. 7 describes T-type thermocouples and the wind sensor model MD0550 from Modern Device, which are installed at eight locations on the evaporator and condenser airstreams. Also, The Data Acquisition (DAQ) system is used to collect data from the thermocouples, pressure transducers, DC power supply, and flow meters, and this data is sent to a computer. LABVIEW is employed to obtain all the measured data from the equipment and to save it in an EXCEL file.

The two fans of the evaporator and condenser are controlled by two VFDs such that the speed could be represented by frequency. While the compressor only has three different speeds, an NI relay module (NI9485) is used to switch between the three discrete speeds.

5. Controller development and implementation

5.1. On/off controller

The on/off controller is most commonly used in vapor compression units because of its simplicity. However, it has many drawbacks as mentioned in the previous sections. Therefore, the on/off controller developed in this section serves simply as a basis of comparison for new controllers. The on/off control strategy is actually a simple hysteresis where the hysteresis band is used to reduce the compressor's frequent switching. When the system is on, the compressor is running at maximum speed. The controller is driven by the error signal between the measured temperature and the temperature set point in the cargo space [49].

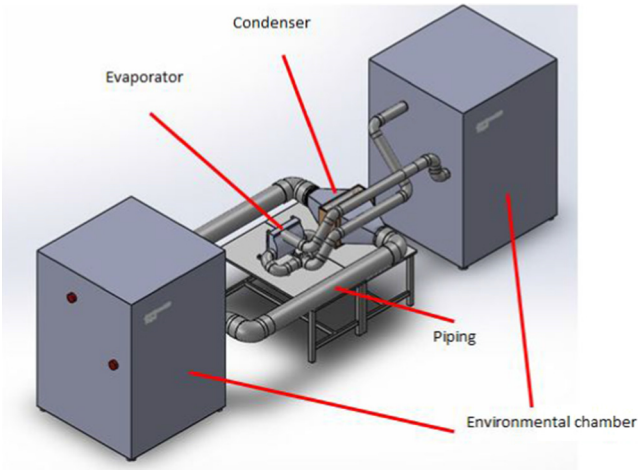

Fig. 2. Schematic of the experimental system.

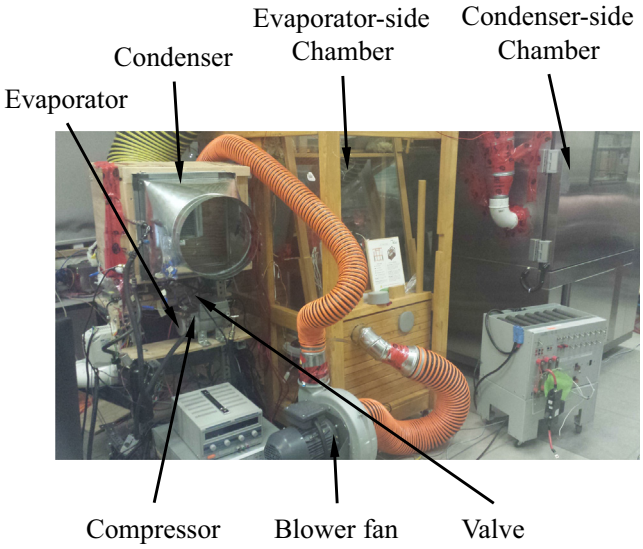

Fig. 3. Experimental system.

Fig. 5. Refrigerant mass flow meter.

Fig. 4. Chamber.

Fig. 6. Thermocouple & pressure transducer.

The controller was built in MATLAB/SIMULINK and LABVIEW for simulation and experiment, respectively. Due to the slow dynamics of the A/C-R system, the control & simulation loop is employed in the control design & simulation module instead of the real-time module; whereas, the simulation time, step size, and timing source are set up to guarantee that the controllers run in real time.

5.2. MPC

As an optimal control method, the MPC originated in the chemistry industry's control techniques. It is characterized by its slow dynamics, which provides enough time for optimization calculations [50]. As is known, the A/C-R system is a highly nonlinear MIMO system with slow dynamics making it suitable for MPC application. In general, three parts are included in an MPC: a predictive model that aims to predict future behavior of the process, a receding horizon optimization algorithm that will solve an explicit optimization problem formulated into several future sampling

Fig. 7. Air temperature & velocity sensors.

periods, and feedback correction to keep the controlled variables at the set points and enhance the robustness of the A/C-R control system [51].

Using a highly complex nonlinear model for the development of a model predictive controller, the computational efficiency will be extremely low, so its real-time implementation will become expensive or even unrealistic for industrial applications. To solve this problem, a linear MPC will be developed in this paper. After linearizing and discretizing the nonlinear model [52], a finite horizon optimization problem [53] is formulated at each time interval. The objective function is shown below,

$$J(x_0,u_0)=e(N)^T Pe(N)+\sum_{k=0}^{N-1}\left[e(k)^T Qe(k)+u(k)^T Ru(k)+\Delta u(k)^T S\Delta u(k)\right]$$

$$s.t.$$

$$x_{min}\leqslant x(k)\leqslant x_{max},\quad k=0,\ldots N-1$$

$$u_{min}\leqslant u(k)\leqslant u_{max},\quad k=0,\ldots N-1$$

$$\Delta u_{min}\leqslant \Delta u(k)\leqslant \Delta u_{max},\quad k=0,\ldots N-1 \tag{11}$$

where e is the tracking error of the temperature; the first term on the right-hand side is the terminal cost; the second term is stage cost; the third term represents control effort cost and the last term is control input rate costs. P, Q, R, and S are weights to balance each term. The objective function is transferred into a quadratic form with respect to the increment of control inputs. As the prediction horizon length is N, the deviation trajectory of future states will be obtained by the discrete model:

$$\underbrace{\begin{bmatrix}\Delta x(1)\\ \Delta x(2)\\ \vdots\\ \Delta x(N)\end{bmatrix}}_{\Delta\overline{X}}=\underbrace{\begin{bmatrix}A\\ A^2\\ \vdots\\ A^N\end{bmatrix}}_{S^{\Delta x}}\Delta x(0)+\underbrace{\begin{bmatrix}B & 0 & \ldots & 0\\ AB & B & \ldots & 0\\ \vdots & \vdots & \ddots & 0\\ A^{N-1}B & A^{N-2}B & \ldots & B\end{bmatrix}}_{S^{\Delta u}}\underbrace{\begin{bmatrix}\Delta u(0)\\ \Delta u(1)\\ \vdots\\ \Delta u(N-1)\end{bmatrix}}_{\Delta\overline{U}} \tag{12}$$

Then, the deviation of the future outputs can be rewritten into a compact form by:

$$\underbrace{\begin{bmatrix}\Delta y(1)\\ \Delta y(2)\\ \vdots\\ \Delta y(N)\end{bmatrix}}_{\Delta\overline{Y}}=\underbrace{\begin{bmatrix}C & 0 & 0 & 0\\ 0 & C & 0 & 0\\ 0 & 0 & \ddots & 0\\ 0 & 0 & 0 & C\end{bmatrix}}_{C^{\Delta x}}\Delta\overline{X} \tag{13}$$

The convex quadratic objective function only with respect to the increment of inputs will be obtained by inserting Eq. (13) into the original objective function shown in Eq. (11) and neglecting the constant term:

$$J(x_0,u_0)=\frac{1}{2}\Delta\overline{U}^T H\Delta\overline{U}+\Delta\overline{U}^T g$$

$$H=2\left(C^{\Delta X}S^{\Delta U}\right)^T\overline{Q}\left(C^{\Delta X}S^{\Delta U}\right)+\overline{R}+\overline{S},g=2\left(C^{\Delta x}S^{\Delta u}\right)^T\overline{Q}\left(C^{\Delta x}S^{\Delta u}-\overline{Y}_{ref}\right)$$

$$s.t.$$

$$\Delta\overline{U}\geqslant max\left(\Delta\overline{U}_{min}(U),\Delta\overline{U}_{min}(\Delta\overline{U}),\Delta\overline{U}_{min}(X)\right)$$

$$\Delta\overline{U}\leqslant min\left(\Delta\overline{U}_{max}(U),\Delta\overline{U}_{max}(\Delta\overline{U}),\Delta\overline{U}_{max}(X)\right) \tag{14}$$

where the Hessian matrix (H) is symmetric and positive or semi-positive definite and g is the gradient vector. $\overline{Q},\overline{R},\overline{S}$ and $\overline{Y}_{ref}$ should be reformulated according to the prediction horizon length N based on Q, R, S and Y_{ref}. The updated constraints of the increment of the control can be found by the reformulation of Eq. (12) and the constraints shown in Eq. (11). For example, the constraints of the states can be applied to $\Delta\overline{U}$ as $\Delta\overline{U}_{max}(X)$ by Eq. (12). Since the optimal result is the small variation $\Delta\overline{U}$, the real optimal $\overline{U}$ can be obtained by adding the initial input U_0. The first element of the optimal solution will be applied to the real system.

This linear MPC is implemented into MATLAB/SIMULINK and LabVIEW for simulation and experiment, respectively. The detailed structure of the MPC in the Control & Simulation Loop in LABVIEW is depicted in Fig. 8. First, the thermodynamic properties, such as density, enthalpy, and entropy, of the refrigerant under the current working conditions are obtained online by feeding the fresh measurements into lookup tables followed by parameter and state identification, where some unknown parameters and states are identified online. Then, all the known information is sent to the MPC algorithm, whose output is a quadratic problem (QP), shown in Eq. (14). A QP open source solver [54], which is originally written in C, is also integrated into the Control & Simulation Loop in LABVIEW and solves the QP at each time interval. The outputs will be delivered to the evaporator and condenser fans as well as the compressor pump via some other NI DAQs control modules to regulate their speeds. If the three control inputs are continuously varying in their ranges, the MPC is the continuous one. Due to the discrete constraint of the compressor speed (i.e. low, medium and high speed), the discrete MPC is designed, where three continuous MPC are employed and solved simultaneously at each time interval. Each of these works at one compressor speed to find the optimum solutions for the other two inputs and the cost values. Then, the three cost values are compared to determine the minimum value, and their three corresponding inputs are used as the optimal solutions.

6. Controller tuning and performance comparison

In this section, the controller's performance is compared in terms of both controlled temperature performance and energy consumption. To study the A/C-R energy consumption at different ambient temperatures, the condenser is connected to an environmental chamber whose temperature is controlled. Three different ambient temperatures [20 °C;25 °C;30 °C] are chosen for the

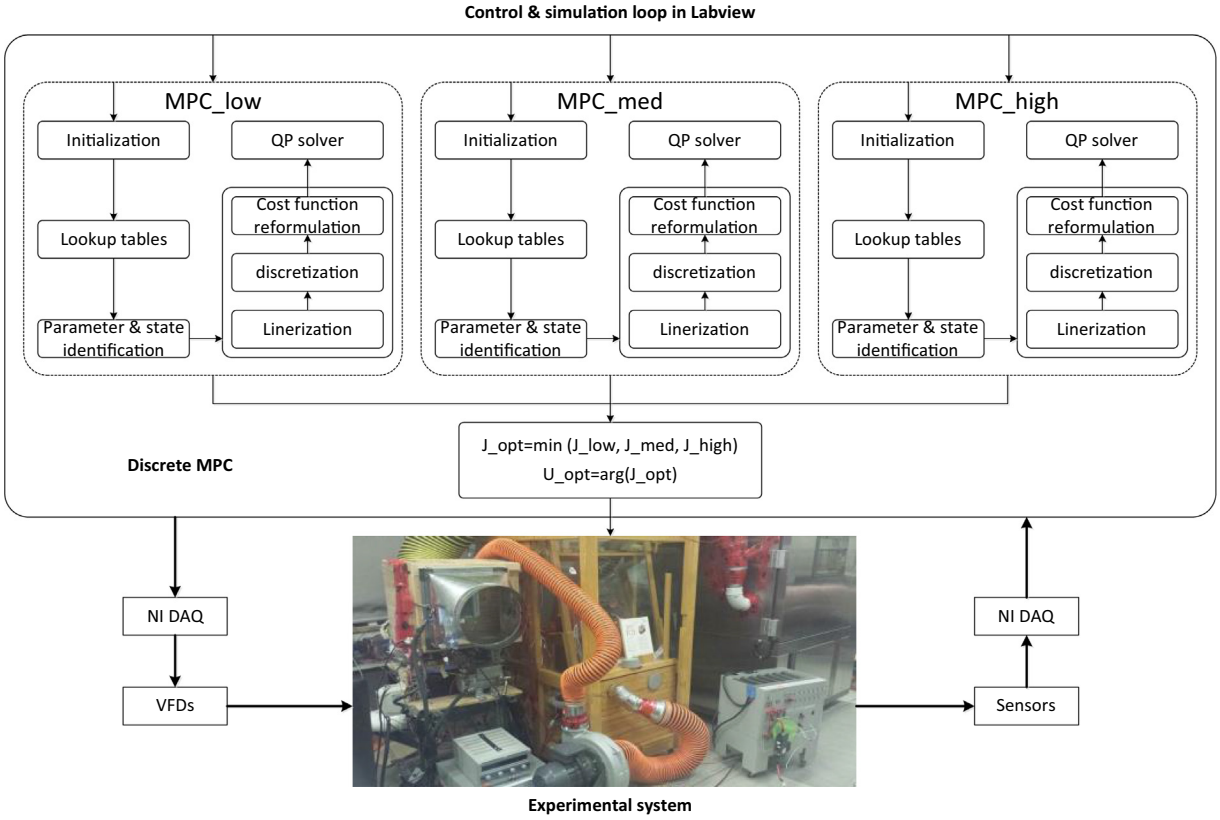

Fig. 8. Discrete MPC structure in LabVIEW.

experiments. The cargo used in the experiments is a 2 m^3 wooden chamber shown in Fig. 4. There are 15 thermocouples to measure the temperature at different locations. For the experiments, an average temperature of 7 thermocouples closer to the air inlet of the condenser was used as the controlled temperature. The hysteresis band is an important parameter in the on/off controller, which should be determined before running the simulation. It decides the temperature oscillation and switching frequency of the whole cycle and subsequently, the wear condition of the compressor. Therefore, for the sake of a trade-off between the two aspects, ±1 °C is chosen as the band by the preliminary experiment study. Under different ambient temperature conditions, the A/C-R system runs at maximum capacity until the chamber temperature stabilizes. Three different temperatures [16 °C;17 °C;18 °C] are chosen as the temperature set points of the air inside the cargo. Furthermore, the on/off threshold should be determined before testing the on/off controller. If the threshold is too large, the temperature variation amplitude is too large. Otherwise, the system will be switched on and off too frequently. After these two aspects are taken into account and some preliminary tests are performed, a ±1 °C threshold is chosen. Table 1 shows the operating conditions and system constraints for both experiment and simulation.

6.1. On/off controller

For the controller performance analysis, several experiments in different scenarios are performed. In order to demonstrate the performance of the controller, the test results under the operating condition mentioned in Table 1 are provided.

During the tests, an external disturbance of approximately 23% of the original heating load (the 200-s disturbed region shown in Fig. 9) was applied to the chamber to simulate the disturbance caused by an opening door. Figs. 9 and 10 refer to the state and input responses of the system, respectively.

6.2. Discrete MPC

In this section, the controller parameters are briefly discussed and chosen. As the sample time T_s decreases, the ability to reject disturbance improves, but the computational effort increases dramatically to guarantee the real-time application. Thus, the best choice is a trade-off between robustness and computational effort based on the dynamics of the system [33,55]. The prediction horizon is related to the size of the quadratic optimization problem (the computational effort) and the accuracy of the prediction. A larger value leads to a better suboptimal solution with much more computational effort and increases the prediction's uncertainties. During the tuning process, N starts with a small value until further increase cannot bring obvious impact on the controller's performance. From Table 1, the scale factors of the three inputs and the output can be set as 2000, 40, 40 and 10, respectively. In order to ensure the value of each term in the objective function in the same scale, a larger Q is chosen. For the weight matrix R of the control effort, a larger weight is selected for the compressor

Table 1
Operating conditions and constraints of inputs and states.

T_{amb} (°C)	T_{cargo_init} (°C)	$T_{setpoint}$ (°C)	$\dot{Q}_{door}$ (kW)	N_{evap} (Hz)	N_{cond} (Hz)	N_{comp} (rpm)	P_c (bar)	P_e (bar)
25	22.5	16	0.15	[0–40]	[0–40]	$\begin{bmatrix}2500\\3500\\4500\end{bmatrix}$	[0–17]	[0.7–7]

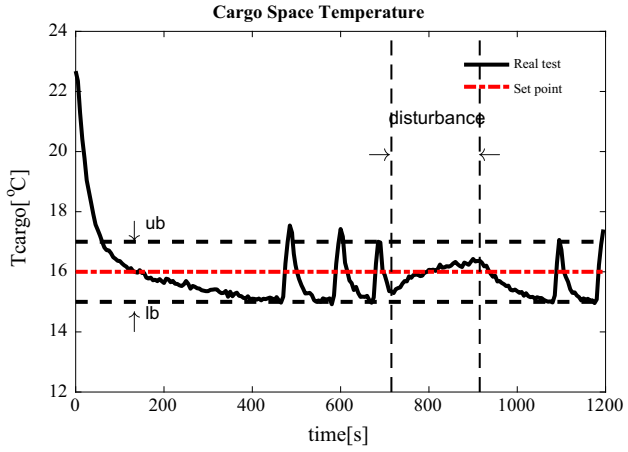

Fig. 9. Temperature performance of on/off controller.

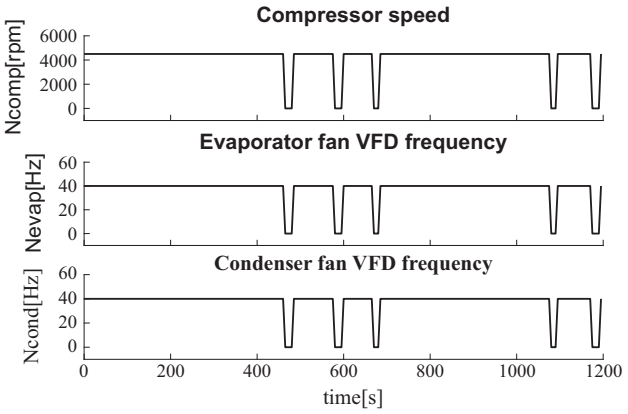

Fig. 10. System inputs of on/off controller.

speed—the most energy-consuming component; whereas, the remaining values are zeros. Usually, the larger input rate weights of S lead to more conservative control moves and produce a more robust performance [55]. By properly choosing a terminal weight from the Riccati equation, a finite-horizon MPC equivalent to an infinite-horizon linear quadratic regulator can be designed to achieve the close-loop stability of the plant [56,57]. If the applications involve constraints, it is difficult to find such a time-varying terminal weight, and it usually needs a terminal constraint to force the plant states into a defined region at the end of horizon [55]. However, as per the tuning guideline suggested in [43], a sufficiently large value of the terminal weight can lead to a better closed-loop performance in most cases. The controller's parameters are presented in Table 2.

Figs. 11 and 12 show that the discrete MPC performs better than the on/off controller. For instance, the MPC controller can keep the temperature of the cargo in a smaller range, compared to ±1 °C of the on/off controller. With the external disturbances up to 23% of the original heating load, the controller will optimally increase the cold air flow rate to balance the extra heating using the evaporator fan to maintain the closed-loop dynamics.

As seen thus far, the MPC has better control performance than the conventional on/off controller because it is able to keep the temperature around its set point with smaller oscillations. In addition, energy consumption serves as the most crucial criterion to show the advantages of the MPC controller. In Table 3, the energy consumption in the 1200 s under the same conditions for each

Table 2
MPC parameter.

$T_s(s)$	N	Q	R	S	P
5	10	100,000	$\begin{bmatrix}5&0&0\\0&0&0\\0&0&0\end{bmatrix}$	$\begin{bmatrix}0&0&0\\0&1000&0\\0&0&1000\end{bmatrix}$	1000Q

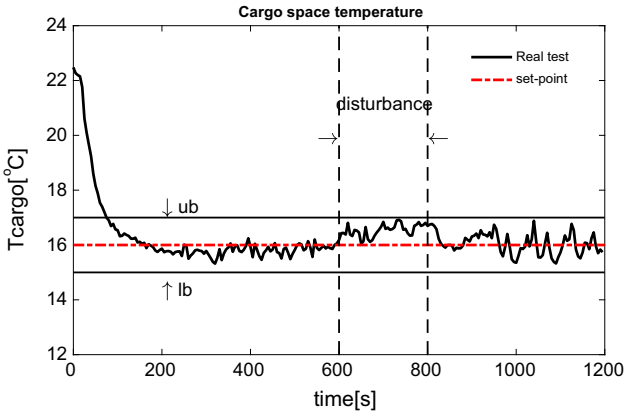

Fig. 11. Temperature performance of discrete MPC.

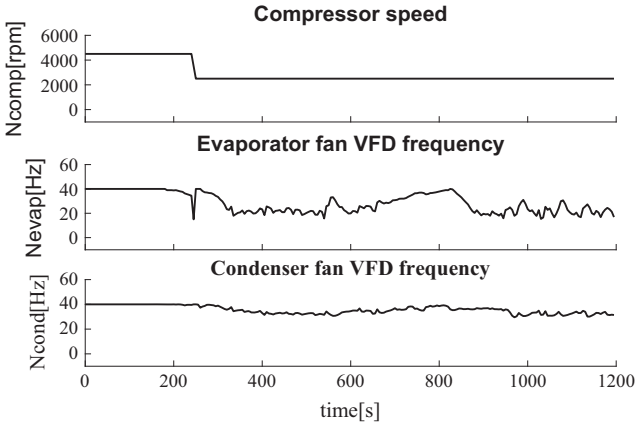

Fig. 12. System inputs of discrete MPC.

controller is given. As expected, the discrete MPC consumes less energy than the on/off controller under the examined scenario.

As mentioned above, a large disturbance is added to the plant and the results show good performance of the proposed controller. As a common phenomenon of the A/C-R system, the frosting problem always exists [58]. When frost appears, it can cause model inaccuracies. For example, the refrigerant mass flow rate through the valve will decrease when the system is frosting, and accordingly, so do many other parameters such as pressures, temperature and superheat. In order to further demonstrate the robustness of the developed controller, the experimental results during the thermostatic expansion valve (TXV) frosting under two cases are presented. Figs. 13 and 14 show the TXV with and without frost.

In the first scenario, the ambient temperature is 25 °C and the temperature set point is 18 °C; whereas, the ambient temperature is set at 30 °C with 16 °C set point in the second scenario. The temperature responses and system inputs are demonstrated in Figs. 15–18, respectively. It can be seen from the figures that the closed-loop performance of this proposed MPC is still satisfactory under both large external disturbances and frosting conditions.

Table 3
Energy consumption of two controllers.

	Energy consumption for 1200s (kW h)	Improvement
On/off	0.2063	Basis
Discrete MPC	0.1902	7.8%

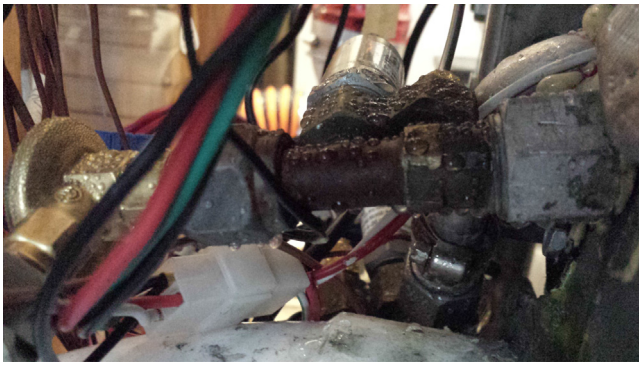

Fig. 13. TXV without frost.

Fig. 14. TXV with frost.

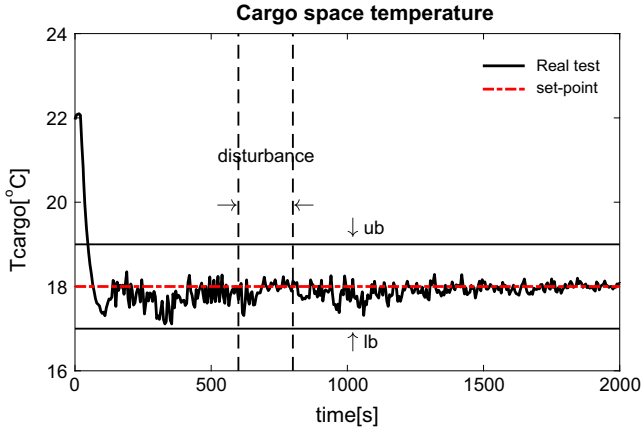

Fig. 15. Temperature performance of discrete MPC under first scenario.

7. Case study

In this last section, the controller's performance and energy-saving benefits are studied under one fixed heating load condition, so in this section, the performance of both controllers are simulated under a time-varying heating load condition. Table 4 shows

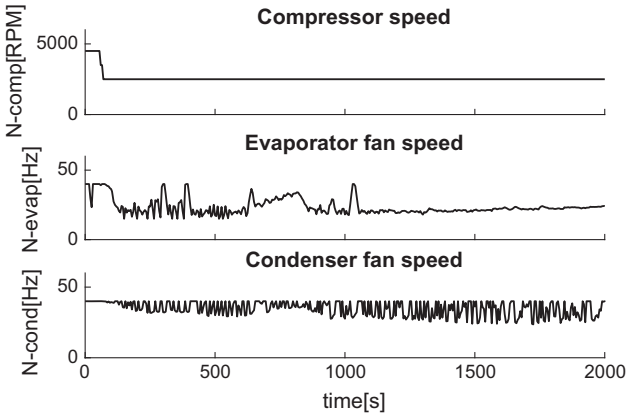

Fig. 16. System inputs of discrete MPC under first scenario.

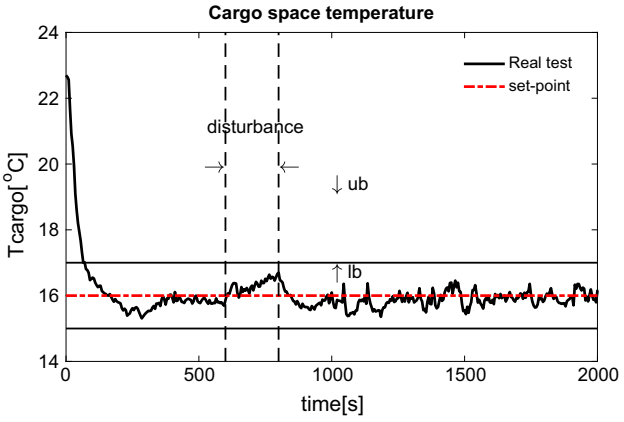

Fig. 17. Temperature performance of discrete MPC under second scenario.

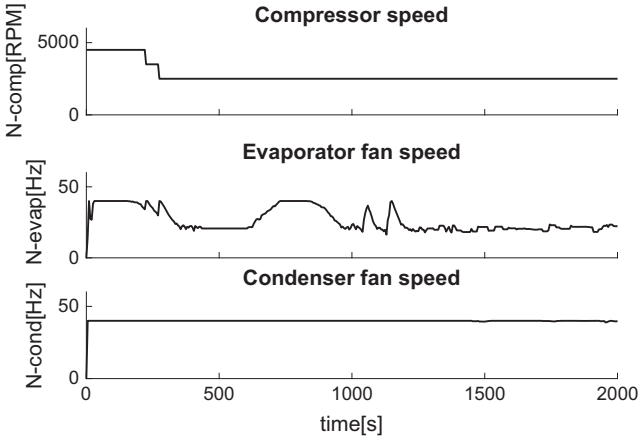

Fig. 18. System inputs of discrete MPC under second scenario.

the energy consumptions of the on/off controller and the discrete MPC under different heating loads. It can be seen that under higher heating load (above 0.5 kW) conditions, the discrete MPC consumes less energy than the on/off controller while for lower heating loads, the on/off controller is more efficient. Thus, it cannot be concluded that the discrete MPC is better than the on/off controller, rather than the discrete MPC could alleviate temperature fluctuations. That is why the other controllers appear in the following sections.

Table 4
Energy consumptions under different heating load conditions.

Heating load (kW)	Energy consumption for 1200s (kW h)	
	On/off	Discrete MPC
0.8	0.2311	0.2119
0.7	0.2162	0.1955
0.6	0.1895	0.1789
0.5	0.1671	0.1657
0.4	0.1451	0.1624
0.3	0.1179	0.1523
0.2	0.0925	0.1343

7.1. Hybrid controllers

By studying the energy consumptions under different heating load scenarios in Table 4, a direct hybrid controller could be intuitively designed by combining the discrete MPC and the on/off controller along with an identifier that could estimate the current heating load. The criterion for activating the discrete MPC is when the heating load is higher than 0.5 kW, and the on/off controller is activated in all other scenarios. Based on the experimental and simulated data, it is known that the cooling capacity produced by the system using the minimum compressor speed can balance the heating load under 0.5 kW. In addition, the compressor is the most energy-consuming component in A/C-R system. As a result, the minimum compressor speed and maximum evaporator and condenser fan speeds are used in this on/off controller.

Even with these parameters, during a low heating load period, the on/off controller will switch the system frequently. In order to alleviate the effects of this phenomenon, an adaptive hybrid controller is given. The main idea is that the system starts working by using the discrete MPC until the controlled temperature settles down at its set point. Then, the MPC is still used as long as the current heating load is over 0.5 kW. Otherwise, the on/off controller will be used. In addition, the speed of the evaporator fan will be updated by:

$$N_{evap} = N_{evap-mpc} + k_{evap}\left(T_{evap-cham} - T_{setpoint}\right) \quad (15)$$

where $N_{evap-mpc}$, is the speed found by the discrete MPC at the switching point; k_{evap}, is a proportional coefficient and related to the switching frequency of the system when using on/off controller. When k_{evap} is zero, this hybrid controller will be the discrete MPC. Otherwise, when it is high enough, it will become the direct hybrid controller.

7.2. Continuous MPC

In some recent applications of the A/C-R system, the continuous variable components instead of components with several different speeds are employed. In order to study the potential of the MPC in these cases, a continuous MPC is designed based on the same model and procedures shown above. In this controller, the input of the compressor speed can continuously change from zero to its maximum speed [48].

7.3. Controllers comparison

In order to compare the controllers discussed above, a heating load cycle shown in Fig. 19 is applied to the system for the simulations. This cycle is used to represent the heating load during a day in 1200 s. As is well-known, the temperature at noon is higher than that in the morning and evening; as such, the heating load applied to the chamber reflects daily temperature variances. Although the heating load changes in a much lower frequency in the real situation, this cycle could also examine the robustness of the controllers.

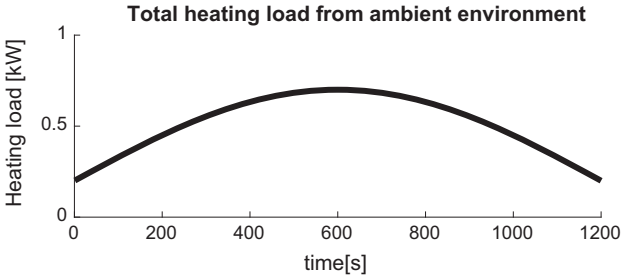

Fig. 19. A heating load pattern.

Fig. 20 shows the system inputs of the on/off controller. The system stays on for a longer period of time under the large heating load condition and vice versa. The controlled temperature behavior and total energy consumption are provided in Fig. 21. The energy consumption will be also used as a basis of comparison for the following controllers.

The system inputs, temperature behavior and energy consumption for the discrete MPC are provided by Figs. 22 and 23.

The results of the direct hybrid controller are shown in Figs. 24 and 25. It can be seen that the on/off controller and the discrete MPC are alternated when the heating load is 0.5 kW.

By choosing 1 as the value of k_{evap}, the results of the adaptive hybrid controller are given in Figs. 26 and 27. These figures show that in comparison to the direct hybrid controller, the lower activation frequency of the system is obtained at the expense of energy

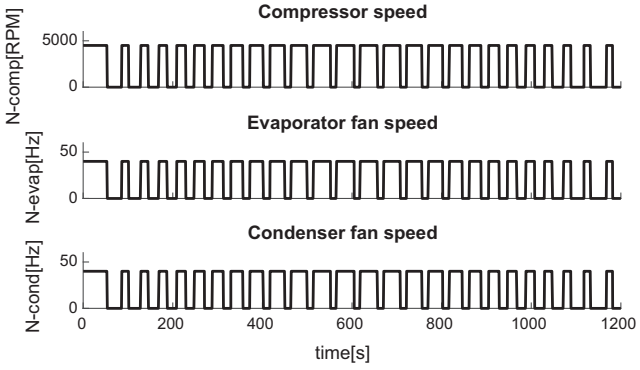

Fig. 20. System inputs of on/off controller.

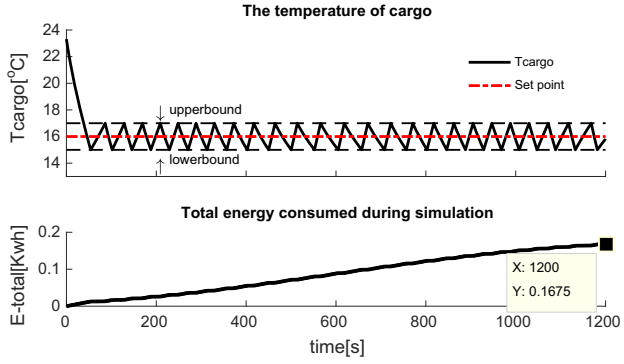

Fig. 21. Temperature performance and energy consumption.

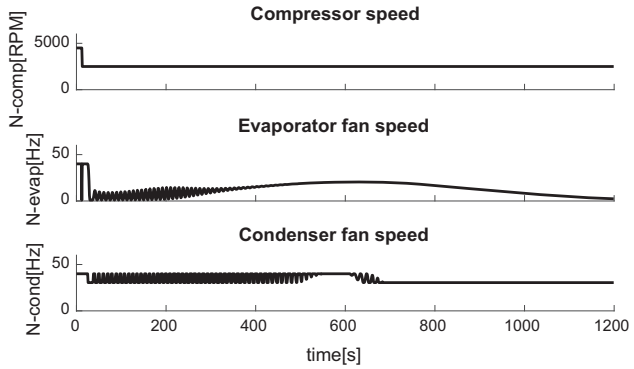

Fig. 22. System inputs of discrete MPC.

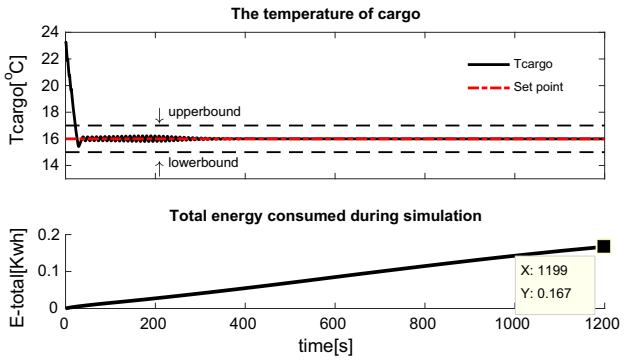

Fig. 23. Temperature performance and energy consumption.

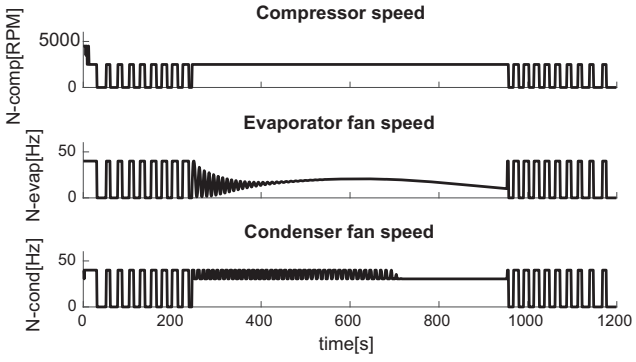

Fig. 24. System inputs of direct hybrid controller.

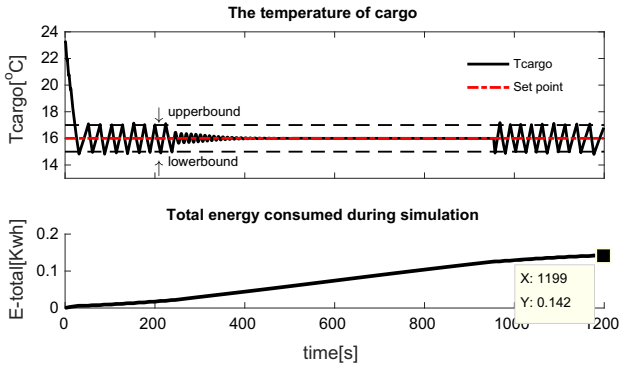

Fig. 25. Temperature performance and energy consumption.

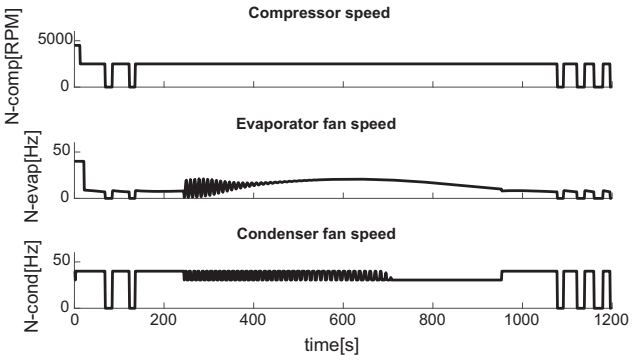

Fig. 26. System inputs of adaptive hybrid controller.

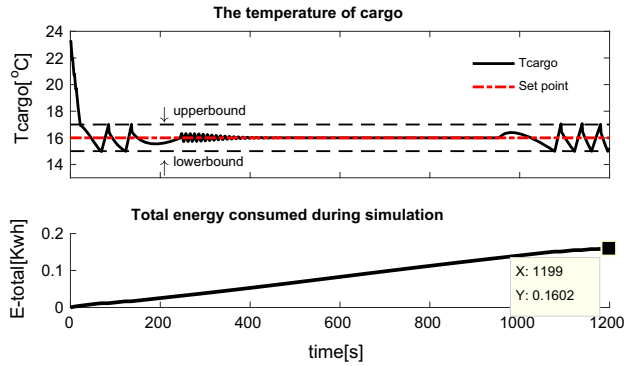

Fig. 27. Temperature performance and energy consumption.

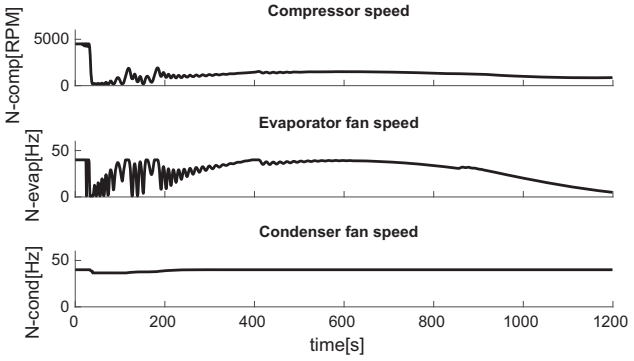

Fig. 28. System inputs of continuous MPC.

consumption. As a result, a trade-off performance between energy consumption and switching frequency of the system can be obtained by using the desired value of k_{evap}.

The controlled temperature performance and energy consumption of the continuous MPC are demonstrated as follows. In Fig. 28, the compressor speed can be manipulated freely according to the changing heating load instead of alternating between several discrete values. In Fig. 29 the temperature response and energy consumption of the continuous MPC are shown.

All the above simulations are done under the same working conditions as given in Table 1 but with the new heating load cycle shown in Fig. 19. The total energy consumption and improvements of the proposed controllers with respect to the conventional on/off controller are listed in Table 5.

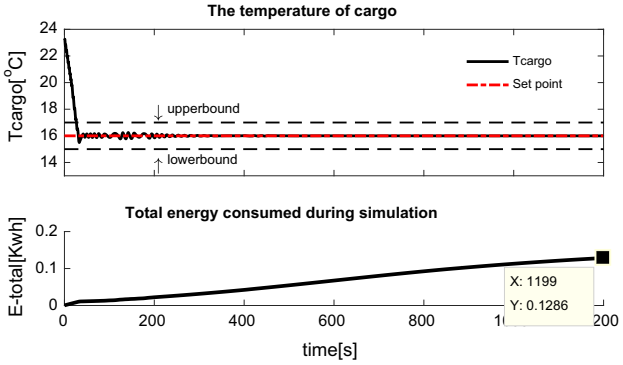

Fig. 29. Temperature performance and energy consumption.

Table 5
Energy consumptions of different controllers.

Controllers	Energy consumption 1200s (kW h)	Improvement (%)
On/off	0.1675	Basis
Discrete MPC	0.1670	0.24
Direct hybrid	0.1420	15.17
Adaptive hybrid	0.1602	4.30
Continuous MPC	0.1286	23.18

8. Discussion and conclusions

The goal of this study was to develop an advanced controller for automotive A/C-R systems, which can not only save energy but also enhance performance.

In this study, a control-based model was proposed and validated by an experimental A/C-R system used in trucks. Then, an on/off controller was designed as a benchmark to demonstrate the improvement of other controllers. Due to the existence of the discrete input of the experimental system, a discrete MPC was designed. The experimental results showed that the model used for controller development is accurate and the discrete MPC not only consumes less energy but also has better temperature behavior than the on/off controller under the examined condition. The robustness of the proposed MPC was also evaluated with the appearance of large external disturbances and the conditions of the plant frosting period. All the test results showed that the MPC is robust. Then, the controller was tested under the time-varying heating load condition. The results also indicated that the discrete MPC uses less energy only under higher heating load conditions. That is why the two hybrid controllers were studied and developed. The direct hybrid combines the energy-saving advantage of the discrete MPC and the on/off controller under all conditions; whereas, the adaptive hybrid controller can reach a balance between energy consumption and component wear. These hybrid controllers are two promising options for the A/C-R systems with discrete inputs according to the requirements. The continuous MPC was also examined, which is the optimal controller for the A/C-R systems with continuously varying components because it can save up to 23% energy with a satisfactory performance.

In addition, the simulation and experimental analysis demonstrated that the proposed MPCs can be used in real time, and it can also achieve the goals of saving energy and improving performance. Therefore, the developing process and modeling method of the MPC can be applied to other complex plants. Future studies will focus on integrating the power consumption model of the whole system into the objective function instead of only control efforts, designing a fully controllable experimental system to test the proposed continuous MPC controller, and implementing the controller into a real vehicle to test its performance in practice.

Acknowledgements

The authors would like to acknowledge the financial support of Automotive Partnership Canada (APC) and the financial and technical support of Cool-it Group.

References

[1] Sorrentino M, Rizzo G, Sorrentino L. A study aimed at assessing the potential impact of vehicle electrification on grid infrastructure and road-traffic greenhouse emissions. Appl Energy 2014;120:31–40.
[2] Wang H, Huang Y, Khajepour A, Song Q. Model predictive control-based energy management strategy for a series hybrid electric tracked vehicle. Appl Energy 2016;182:105–14.
[3] Chua KJ, Chou SK, Yang WM, Yan J. Achieving better energy-efficient air conditioning – a review of technologies and strategies. Appl Energy 2013;104:87–104.
[4] Khayyam H, Abawajy J, Jazar RN. Intelligent energy management control of vehicle air conditioning system coupled with engine. Appl Therm Eng 2012;48:211–24.
[5] Oh MS, Ahn JH, Kim DW, Jang DS, Kim Y. Thermal comfort and energy saving in a vehicle compartment using a localized air-conditioning system. Appl Energy 2014;133:14–21.
[6] Huang Y, Khajepour A, Wang H. A predictive power management controller for service vehicle anti-idling systems without a priori information. Appl Energy 2016;182:548–57.
[7] Hu X, Johannesson L, Murgovski N, Egardt B. Longevity-conscious dimensioning and power management of the hybrid energy storage system in a fuel cell hybrid electric bus. Appl Energy 2015;137:913–24.
[8] Sun F, Hu X, Zou Y, Li S. Adaptive unscented Kalman filtering for state of charge estimation of a lithium-ion battery for electric vehicles. Energy 2011;36(5):3531–40.
[9] Hu X, Li SE, Jia Z, Egardt B. Enhanced sample entropy-based health management of Li-ion battery for electrified vehicles. Energy 2014;64:953–60.
[10] Budde-Meiwes H et al. A review of current automotive battery technology and future prospects. Proc Inst Mech Eng, Part D: J Automob Eng 2013;227(5):761–76.
[11] Huang Y, Khajepour A, Bagheri F, Bahrami M. Modelling and optimal energy-saving control of automotive air-conditioning and refrigeration systems. Proc Inst Mech Eng, Part D: J Automob Eng 2016.
[12] Leva A, Piroddi L, Di Felice M, Boer A, Paganini R. Adaptive relay-based control of household freezers with on–off actuators. Contr Eng Pract 2010;18(1):94–102.
[13] Li B, Otten R, Chandan V, Mohs WF, Berge J, Alleyne AG. Optimal on–off control of refrigerated transport systems. Contr Eng Pract 2010;18(12):1406–17.
[14] Liu J, Zhou H, Zhou X. Automotive air conditioning control – a survey. In: International conference on electronic & mechanical engineering and information technology, EMEIT 2011, Harbin, Heilongjiang, China.
[15] Høgh G, Nielsen R. Model based nonlinear control of refrigeration systems. M.S. thesis, section for automation and control. DK - 9100 Aalborg, Denmark: Aalborg University; 2008.
[16] Afram A, Janabi-Sharifi F. Theory and applications of HVAC control systems – a review of model predictive control (MPC). Build Environ 2014;72:343–55.
[17] Petersen A, Lund P. Modeling and control of refrigeration systems. M.S. thesis, Institute of Electronic Systems. DK - 9100 Aalborg, Denmark: Aalborg University; 2004.
[18] Li N, Xia L, Shiming D, Xu X, Chan M-Y. Dynamic modeling and control of a direct expansion air conditioning system using artificial neural network. Appl Energy 2012;91(1):290–300.
[19] Mohanraj M, Jayaraj S, Muraleedharan C. Applications of artificial neural networks for refrigeration, air-conditioning and heat pump systems—a review. Renew Sustain Energy Rev 2012;16(2):1340–58.
[20] Koo B, Yoo Y, Won S. Super-twisting algorithm-based sliding mode controller for a refrigeration system. In: Control, automation and systems (ICCAS), 2012 12th international conference on. IEEE; 2012. p. 34–8.
[21] Shah R, Alleyne AG, Bullard CW, Rasmussen BP, Hrnjak PS. Dynamic modeling and control of single and multi-evaporator subcritical vapor compression systems. Air Conditioning and Refrigeration Center. College of Engineering. University of Illinois at Urbana-Champaign; 2003.
[22] Rasmussen BP, Alleyne AG. Dynamic modeling and advanced control of air conditioning and refrigeration systems. Air Conditioning and Refrigeration Center. College of Engineering. University of Illinois at Urbana-Champaign; 2006.
[23] He XD. Dynamic modeling and multivariable control of vapor compression cycles in air conditioning systems. PhD thesis. USA: Massachusetts Institute of Technology; 1996.
[24] He X-D, Liu S, Asada H, Itoh H. Multivariable control of vapor compression systems. HVAC&R Res 1998;4(3):205–30.

[25] Larsen LFS. Model based control of refrigeration systems. PhD thesis. DK - 9100 Aalborg, Denmark: Department of Control Engineering, Aalborg University; 2006.
[26] Sousa JM, Babuška R, Verbruggen HB. Fuzzy predictive control applied to an air-conditioning system. Contr Eng Pract 1997;5(10):1395–406.
[27] He M, Cai W, Li S. Multiple fuzzy model-based temperature predictive control for HVAC systems. Inf Sci 2005;169(1–2):155–74.
[28] Razi M, Farrokhi M, Saeidi MH. Neuro-predictive control for automotive air conditioning system. In: Engineering of intelligent systems, IEEE international conference on. IEEE; 2006. p. 1–6.
[29] Elliott MS, Rasmussen BP. Model-based predictive control of a multi-evaporator vapor compression cooling cycle. In: American control conference. IEEE; 2008. p. 1463–8.
[30] Huang G, Dexter AL. Realization of robust nonlinear model predictive control by offline optimisation. J Process Control 2008;18(5):431–8.
[31] Jain N, Alleyne AG. Thermodynamics-based optimization and control of vapor-compression cycle operation: optimization criteria. In: American control conference (ACC), 2011. IEEE; 2011. p. 1352–7.
[32] Ma J, Qin J, Salsbury T, Xu P. Demand reduction in building energy systems based on economic model predictive control. Chem Eng Sci 2012;67 (1):92–100.
[33] Gustavsson A. Dynamic modeling and Model Predictive Control of a vapor compression system. PhD thesis. Department of Electrical Engineering, Automatic Control. Linköping University, The Institute of Technology, Linköping University; 2012.
[34] Hovgard TG, Larsen LF, Bagterp J, Boyd JS. Fast nonconvex model predictive control for commercial refrigeration; 2012. <https://stanford.edu/~boyd/papers/pdf/noncvx_mpc_refr_nmpc.pdf>.
[35] Yudong, Borrelli F, Hencey B, Coffey B, Bengea S, Haves P. Model predictive control for the operation of building cooling systems. IEEE Trans Control Syst Technol 2012;20(3):796–803.
[36] Blanchin F, Ukovich W. Linear programming approach to the control of discrete-time periodic systems with uncertain inputs. J Optim Theory Appl 1993;78(3):523–39.
[37] Aswani A, Master N, Taneja J, Culler D, Tomlin C. Reducing transient and steady state electricity consumption in HVAC using learning-based model-predictive control. Proc IEEE 2012;100(1):240–53.
[38] Elliott MS, Rasmussen BP. Decentralized model predictive control of a multi-evaporator air conditioning system. Contr Eng Pract 2013;21(12):1665–77.
[39] Sørensen KK, Stoustrup J, Bak T. Adaptive MPC for a reefer container. Contr Eng Pract 2015;44:55–64.
[40] Sarabia D, Capraro F, Larsen LFS, de Prada C. Hybrid NMPC of supermarket display cases. Contr Eng Pract 2009;17(4):428–41.
[41] Sonntag C. Control of a supermarket refrigeration system, HYCON WP4b/WP2, Department of Biochemical and Chemical Engineering Process Dynamics and Operations Group (DYN), HYCON Workshop Brussels; 2009.
[42] Patel T, Shah J, Satria M. Dynamic modeling, optimal control design and comparison between various control schemes of home refrigerator; 2013.
[43] Fagiano L, Teel AR. Generalized terminal state constraint for model predictive control. Automatica 2013;49(9):2622–31.
[44] Fagiano L, Teel AR. On generalized terminal state constraints for model predictive control; 2013. <http://arxiv.org/abs/1207.0788v2>.
[45] Rasmussen BP, Alleyne AG. Control-oriented modeling of Transcritical vapor compression systems. J Dyn Syst Meas Contr 2004;126(1):54.
[46] Eldredge BD, Alleyne AG. Improving the accuracy and scope of control-oriented vapor compression cycle system models. Air Conditioning and Refrigeration Center. College of Engineering. University of Illinois at Urbana-Champaign; 2006.
[47] Zhao D, Tan G. Numerical analysis of a shell-and-tube latent heat storage unit with fins for air-conditioning application. Appl Energy 2015;138:381–92.
[48] Huang Y, Khajepour A, Khazraee M, Bahrami M. A comparative study of the energy-saving controllers for automotive air-conditioning/refrigeration systems. J Dyn Syst Meas Contr 2016;139(1):014504.
[49] Li B. Dynamic modeling and control of vapor compression cycle systems with shut-down and start-up operations. MASc thesis. Air Conditioning and Refrigeration Center, College of Engineering, University of Illinois at Urbana-Champaign; 2009.
[50] Serrao L, Onori S, Rizzoni G. A comparative analysis of energy management strategies for hybrid electric vehicles. J Dyn Syst Meas Contr 2011;133 (3):031012.
[51] Grüne L, Pannek J. Nonlinear model predictive control-theory and algorithms. © Springer-Verlag London Limited; 2011.
[52] Huang Y. Anti-idling systems for service vehicles with A/C-R units: modeling, holistic control, and experiments. Ph.D. Thesis. ON, Canada: Mechanical and Mechatronics Department, University of Waterloo; 2016.
[53] Borrelli F, Bemporad A, Morari M. Predictive control for linear and hybrid systems; 2014. <http://control.ee.ethz.ch/~stdavid/BBMbook_Cambridge_newstyle.pdf>.
[54] Ferreau HJ, Kirches C, Potschka A, Bock HG, Diehl M. QpOASES: a parametric active-set algorithm for quadratic programming. Math Program Comput 2014;6(4):327–63.
[55] Bemporad A, Morari M, Ricker NL. Model predictive control toolbox 3 user's guide. The mathworks; 2010.
[56] Scokaert POM, Rawlings JB. Constrained linear quadratic regulation. IEEE Trans Autom Control 1998;43(8):1163–9.
[57] Jain N, Burns DJ, Di Cairano S, Laughman CR, Bortoff SA. Model predictive control of variable refrigerant flow systems. The international refrigeration and air conditioning conference; 2014.
[58] Tian C, Li X, Yang X. Numerical analysis of evaporator frosting in automotive air-conditioning system with a variable-displacement compressor. Appl Energy 2005;82(1):1–22.